VARIATION OF FLUIDELASTIC CRITICAL VELOCITY WITH MASS RATIO AND REYNOLDS NUMBER IN A DENSELY PACKED NORMAL TRIANGULAR TUBE ARRAY

Stephen Gillen & Craig Meskell
Department of Mechanical Engineering, Trinity College, Dublin

ABSTRACT

Investigation of steady flow through a normal triangular tube bundle is carried out numerically using a 2D Reynolds Averaged Navier-Stokes solver. A single tube of 38mm diameter in the centre of a 1.32 pitch to diameter ratio array is statically displaced and fluid force coefficients on the tube in the centre of the array are obtained for a range of Reynolds number. Comparison of pressure coefficient with experimental data indicates simulations provide a reliable indication of Reynolds number dependance. These fluid force coefficients are then used as input into the quasi-unsteady model in order to predict the critical velocity of damping controlled fluidelastic instability for a single degree of freedom tube within an array. The predicted critical velocities are in the range of empirical data from the literature. It is shown that Reynolds Number has a significant effect on critical velocity. Furthermore the mass ratio can also impact on the critical velocity at high mass-damping values.

1. INTRODUCTION

Flow-induced vibration (FIV) can be a major problem in large heat exchangers leading to them being shut down for repairs or even needing to be replaced outright. This in turn leads to huge losses in revenue as well as the possibility of power outages.

One well recognised form of this vibration is fluidelastic instability, FEI, which is the most destructive and least well understood. Damping controlled FEI can occur even when a single flexible tube, within an otherwise rigid array, is subjected to cross flow. Through a feedback mechanism of negative damping the tube may experience large amplitude self-excited oscillations. The potentially catastrophic nature of this FIV mechanism has lead to a substantial research effort including empirical studies and the development of various models to predict the critical onset velocity.

Tanaka and Takahara (1981) proposed an empirical model in which the fluidelastic force E is represented by various fluid force terms linked with nondimensional coefficients, the values for these coefficients must then be obtained from full dynamic experimental tests. This approach has been used by other researchers (Chen et al, 1994; Meskell and Fitzpatrick, 2003). However it gives little understanding of the fundamentals behind the fluidelastic force.

A theoretical model was proposed by Lever and Weaver (1986) which used redistribution of streamtube area to predict the onset of instability, this model required some empirical input, with a crucial variable being the phase lag term.

The model developed by Price and Paidoussis (1984) used the quasi-steady assumption that the dynamic fluid forces are related to the forces for a statically displaced tube by a phase lag term. This was later developed by Granger and Paidoussis (1996) to represent the phase lag term as a function rather than a constant, which is a more realistic approach. Using this method stability maps were obtained for two array geometries.

Validation of these models is still based primarily on comparison of predicted stability maps with experimental critical velocities. However, the experimental data shows significant unexplained scatter for the values of critical velocity and this is compounded by the lack of fundamental understanding of the fluid dynamics at play.

Previous models have assumed that the effect of Reynolds number has no effect on levels of critical velocity. However, in a limited experimental study Mewes and Stockmeier (1991) have shown this not to be necessarily the case. Price (2001) in his discussion of the applicability of the Connors' equation noted that a complete model of fluidelastic instability should also include a Reynolds number dependency.

In this study the issue of scatter among the experimental data will be investigated as well as the effect of mass ratio. Also the novel approach

of using CFD to obtain the force coefficients, previously obtained experimentally, will be used.

2. THEORY

The fluidelastic force E that a tube in an array is subjected to can be expressed by the governing equation of motion

$$m_s\ddot{y} + c_s\dot{y} + k_s y = E(y, \dot{y}, \ddot{y}, U_0) \tag{1}$$

here the effects of both turbulent buffeting and vortex shedding have been ignored. There are several models for the this function. One such model proposed by Price and Paidoussis (1984) used the quasi steady approach, which assumes the force at any moment in time on the oscillating tube is equal to the force it would be subjected to for that static displacement, along with a time lag on this force to predict values of critical velocity U_c.

This model was later improved upon by Granger and Paidoussis (1996) to represent the time lag as a delay function within which the core problem is the memory function which describes the relation between the instantaneous fluid forces and the static lift force. In this quasi-unsteady model the unsteady Navier-Stokes equations are considered to ultimately give an expression for the instantaneous lift forces the oscillating tube is subject to

$$F_y(t) = -\frac{1}{2}\rho d^2 L C_M \ddot{y} + \frac{1}{2}\rho U_0^2 L d \left(\frac{\partial C_L}{\partial y} h * y - C_D \dot{y}\right) \tag{2}$$

In which d is the tube diameter, L the tube length, ρ the fluid density, U_0 the freestream velocity, and C_M, C_L and C_D the mass, lift and drag coefficients respectively. The instantaneous tube displacement y is convolved with the delay function h. The drag which would normally only be considered for forces in the x direction is included as due to the quasi-steady assumption it will have an impact on the forces on the y direction. However its influence is minimal when compared to the influence of the lift. The convolution integral is given as

$$h * y = \int_0^\tau h(\tau - \tau_0) y(\tau_0) d\tau_0 \tag{3}$$

with h representing the memory function

$$h(\tau) = \frac{d\Phi}{d\tau}. \tag{4}$$

The transient evolution of this memory function, which is the fundamental issue behind damping controlled fluidelastic instability, is determined by the function Φ which converges towards 1 as τ approaches infinity. The chosen representation for this was a series of decaying exponentials, based on Schwartz's theorem:

$$\Phi = \left(1 = \sum_{i=1}^{N} \alpha_i e^{-\delta_i \tau}\right) H(\tau). \tag{5}$$

Previously, Granger and Paidoussis (1996) found the parameters α_i and δ_i by carrying out dynamical tests on a displaced tube in an array subject to cross flow and measuring the vibratory response and force coefficients and inputting the data back into a modified equation.

More recently Meskell (2005) has proposed a simple wake model to predict the values of α_i and δ_i and thus calibrate the model without need for experimental data. This model is built around the assumption that the memory function is the normalized instantaneous bound circulation on the tube. Modelling the wake as a discretizised vortex sheet an equation for the memory function is achieved. From this and by solving the equation of motion in the Laplace domain a quintic polynomial in the critical velocity is obtained.

$$\sum_{i=1}^{5} p_i U_c^i = 0 \tag{6}$$

in which $p_i = p_i(\zeta_0, m_r, C_D, \frac{\partial C_L}{\partial y}, \alpha_1, \alpha_2, \delta_1, \delta_2)$ Using this model the only required input data for the model to predict critical velocities are the structural properties ζ_0 the damping ratio, and m_r the mass ratio, along with the static fluid force coefficients C_D and $\frac{\partial C_L}{\partial y}$. Up until now these force coefficients have been obtained experimentally procedure. This study will obtain these fluid force coefficients through the used of numerical simulation.

3. CFD MODELLING

The array modelled is a rotated triangular arrangement with pitch to diameter ratio (P/d) of 1.32, tube diameter of 38mm and the total width of section is 300mm, which corresponds to the experimental setup in order to facilitate validation. Also by modeling a wide array artificial blockage effects can be avoided, the modelled array arrangement can be seen in figure 1.

The simulations only consider displacement of the central tube on the third row, as this is typical of a tube in the centre of a bundle. The sides

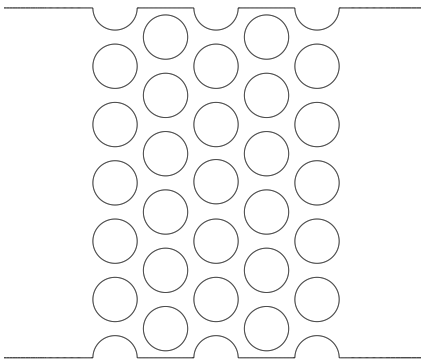

Figure 1: *Schematic of normal triangular tube array of P/d=1.32.*

are modelled as no-slip walls in order to accurately replicate the experimental setup.

The mesh is divided into hexagonal regions around each tube, the detail of which can be seen in figure 2.

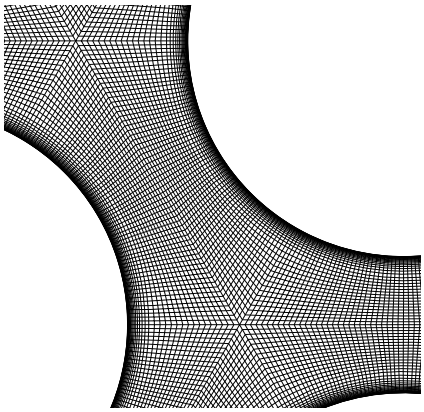

Figure 2: *Detail of hexagonal structure of grid.*

This approach has the advantage that it allows for a much more structured mesh around the tubes, by splitting each into distorted quadrilateral shapes, it can then be easily populated with a structured mesh of quadrilateral cells, over which the user has a large amount of control. It also allows for the displacement of a single tube without need for the whole mesh to be regenerated. For the rest of the domain(i.e. outside the array) triangular cells were used as these allowed for easy meshing of regions with cell size gradients, thus leading to a computationally less expensive simulation.

Within the array 360 cells of equal circumferential length are used around each tube along with boundary layer cells on the surface with an initial thickness of 0.01mm and growth factor of 1.2 this allowed for accurate numerical analysis of this critical region in which velocity gradients are large. Outside of the boundary layer region cells of approximately 0.5mm size were used. The fluid domain extends over 30 tube diameters to the rear and 10 tube diameters to the front to ensure the outflow and velociy inlet boundary condition effects are minimised.

The CFD package Fluent 6.2 was used to perform the simulation using a Reynolds Averaged Navier-Stokes solver. The realizable k-ϵ turbulence model was used in order to attain turbulence closure.

Simulations were carried out for the tube displaced to 1mm for a range of Reynolds number. A 1mm displacement was used as it corresponds to a vibration ampitude of under 2%, which is a realistic limit on tube vibration fot critical velocity (Weaver and Yeung, 1984). The variation of Reynolds number was for the most part achieved by varying the value of fluid viscosity and using a constant inlet velocity of 10m/s. Simulations were also run in which the velocity was modified in order to investigate how well correlated these results were and show that the scaling of force coefficients is with Reynolds number and not just one of its variables. Table 1 summarizes the range of Reynolds numbers tested, as well as the values of U_0 and μ that were used whilst holding the others constant to achieve this. It was found that despite the high mesh density, over 600000 cells, the simulations ran within a reasonable timescale.

Re	$U_0(m/s)$	$\mu(kg/ms) \times 10^{-6}$
13007	5	35.8
15608	6	29.8
18210	7	25.6
20811	8	22.4
23412	9	19.9
26014	10	17.9
28615	11	16.3
31217	12	14.9
33818	13	13.8
36420	14	12.8
39021	15	11.9
41622	16	11.2
44224	17	10.5
46825	18	9.94
49427	19	9.42
52028	20	8.95

Table 1: *Values of U_0 and μ simulations were run for.*

4. RESULTS

4.1. Validation

Two methods were used to validate the results. Firstly the pressure distribution around the displaced tube was compared with data obtained experimentally (Mahon, 2007), it can be seen in figure 3 that there is good correlation between the two results right around the circumference of the tube. The angle is defined by starting at the front of the tube and moving clockwise around it. As can be seen the static pressure is lowest at the top and bottom of the tube as would be expected, as this is the region through which the fluid has to flow fastest due to the smaller area. The highest pressure is at the front of the tube and despite the local maxima at the rear of the tube there is still a significant overall drop across the tube giving rise to the drag force. Although it is hard to see due to the relatively small displacement the pressure distribution is not symmetrical. It is this small variation in pressure that gives rise to the lift force on the displaced tube. If the pressure values at various points are compared directly (2) it can be seen that the results are in reasonable agreement.

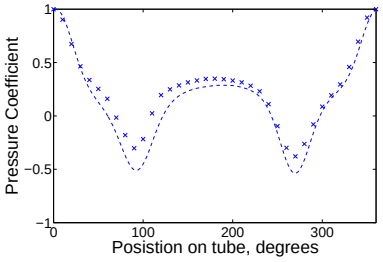

Figure 3: *Pressure Coefficient around tube: —, Numerical data; ×, Experiment data, 10m/s;*

Posistion	Numerical	Experimental
90	-0.504	-0.303
180	0.2851	0.349
270	-0.5371	-0.38

Table 2: *Comparison of Pressure Coefficient .*

The second method of verifying the results is to examine the pressure drop across the array for a range of velocities. Zukaukas (1972) has performed in depth studies into the pressure drop across various arrays and produced empirical relationships for them. When the pressure drop across the array is compared with the results predicted by Zukaukas the correlation is good as can be seen in figure 3 with all of the predicted results gave slightly higher values of pressure drop. These comparisons with experimental data suggest these relatively inexpensive CFD simulations are reliable.

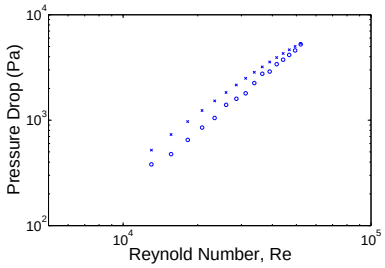

Figure 4: *Comparisson of pressure drop accross array. x, Zukaukas; ∘, Numerical data.*

4.2. Fluid Forces

When the drag force on the displaced tube is extracted and plotted against the freestream velocity on a log log scale the relationship can be easily seen. When a trendline is fitted to the data it indicates that the drag force scale with $U^1.9$ rather than 2 as has been traditionally thought.

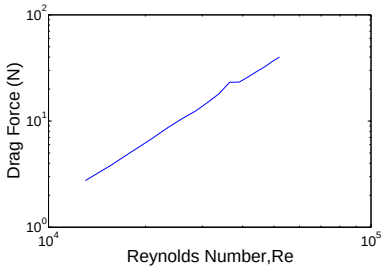

Figure 5: *Variation of Drag force with Reynolds Number.*

This would indicate that the fluid force coefficients due to the pressure distribution around displaced tube (i.e. ignoring viscous forces, which are significantly smaller) are not solely dependant of the dynamic head.

However in the quasi-unsteady model the lift and drag coefficients are used as inputs that scale with Reynolds number as so will be examined. Firstly the coefficient of drag. As can be seen in figure 6 the coefficient of drag varies only slightly with Re, dropping of marginally as Re increases. There is one unexplained spike in the data at a Reynolds number of 36420 though its effect should be minimized due to the small dependance on C_D. The values are marginally higher

than those predicted by Granger and Paidoussis (1996) though due to the fact the drag force has only a minor effect on the predicted values of critical velocity so this should not be a major issue.

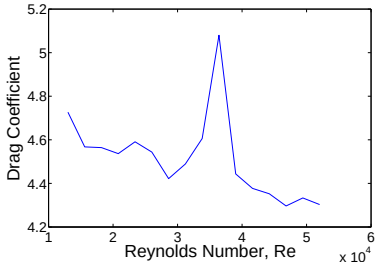

Figure 6: *Variation of Drag Coefficient with Reynolds Number.*

The gradient of the coefficient of lift, $\frac{\partial C_L}{\partial y}$ variation with Reynolds number can be seen in figure 7. The value changes significantly with increasing Reynolds number, reducing nearly an order of magnitude over the range of Reynolds number from 13007 to 52028. Granger and Paidoussis (1996) had used as inputs, values of $\frac{\partial C_L}{\partial y}$ that varied only with P/d.

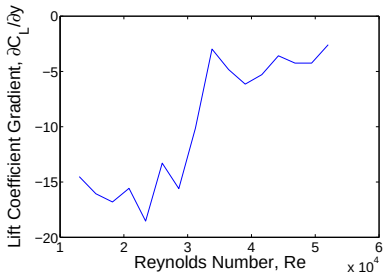

Figure 7: *Variation of Lift Force Coefficient Gradient with Reynolds Number.*

The variation of Reynolds number here was achieved by varying the values of viscosity, however the variation of Reynolds number with changing velocity was also investigated and it was found that similar values of $\frac{\partial C_L}{\partial y}$ were obtained, this would suggest that the scaling is with Re and not just one of its variables. Table 3 shows the comparison between coefficient of lift values for varying velocity and viscosity.

4.3. Application to Quasi-unsteady Model

Using the values for $\frac{\partial C_L}{\partial y}$ and C_d obtained here and the model developed by Meskell (2005) the critical velocity has been calculated for a range of mass ratios and Reynolds number.

Re	Coefficient of lift	
	Viscosity varied	Velocity Varied
13007	-14.5	-14.3
20811	-15.6	-17.9
31217	-10.1	-8.2
41622	-5.3	-5.3
52028	-2.5	-0.6

Table 3: *Comparison of Lift coefficient for varying velocity and viscosity .*

As can be seen in figure 8 in which the critical velocity is plotted against mass damping parameter, for a Reynolds number of 32127, at higher levels of mass damping parameter the mass ratio has a significant effect on the critical velocity, with a increasing mass ratio causing a decrease in critical velocity. However as mass damping parameter increases stiffness-controlled fluidelastic instability will dominate.

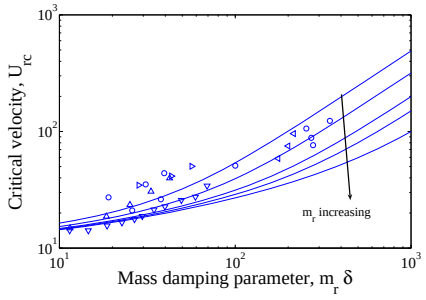

Figure 8: *Variation of Critical Velocity with Mass-damping Parameter for a range of Mass Ratios.*

In figure 9 again critical velocity is plotted against mass damping parameter however this time the effect of variation of Reynolds number is examined. As can be seen the Reynolds number has a significant effect on the critical velocity at all levels of mass damping parameter. An increase in Reynolds number leads to a clear increase in critical velocity. Experimental data from various studies with similar conditions (i.e. single flexible tube in the centre of an otherwise rigid array and similar pitch to diameter ratios) has been overlaid on the graph. The model compares reasonably well with the experimental data suggesting the applicability of CFD for obtaining the required fluid force coefficients. In addition scatter can be seen in the experimental data which has previously had no definitive explanation, It is possible that this scatter is due to variation of Reynolds number

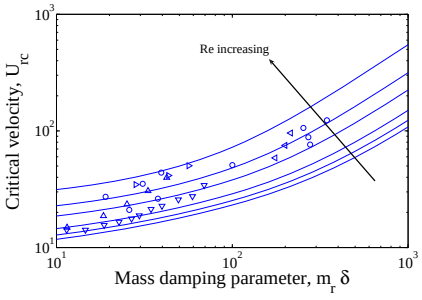

Figure 9: *Variation of Critical Velocity with Mass-damping Parameter for a range of Reynolds Number.*

5. CONCLUSION

Steady flow through a normal triangular array of pitch to diameter ratio of 1.32, with a single displaced tube in centre of array was simulated using a RANS solver. Force coefficients were obtained and used as inputs into the quasi-unsteady model through the use of the simple wake model proposed by Meskell (2005). Stability maps of critical velocity were then created for varying values of Reynolds number and mass-damping parameter.

The predicted stability maps for critical velocity show a significant amount of variation with Reynolds number, and also with mass ratio for higher mass damping parameters, thus indicating that these parameters can not be ignored in analysis of fluidelastic instability.

It was also shown that the inputs for the model obtained from numerical analysis predicted results in the range of experimental values, and so can be concluded that this is a viable method for obtaining these required coefficients

6. ACKNOWLEDGEMENT

This publication has emanated from research conducted with the financial support of Science Foundation Ireland.

7. REFERENCES

Chen, S., Zhu, S., Jendrzejczyk, J., 1994, Fluid damping and fluid stiffness of a tube row in cross-flow. *Journal of Pressure Vessel Technology* **116**: 370-383

Granger, S., Paidoussis, M.P., 1996, An improvement to the quasi steady model with application to crossflow-induced vibration of tube arrays. *Journal of Fluid Mechanics* **320**: 163-184.

Lever, J.H., Weaver, D.S., 1986, On the stability of heat exchanger tube bundles 1: modified theoretical model. *Journal o Sound and Vibration* **107(3)**:375-392.

Mahon, J., 2008, Interaction between Fluidelastic Instability and Acoustic Resonance in normal triangular tube arrays. Ph.D. Thesis

Meskell, C., Fitzpatrick, J.A., 2003, Investigation of the Nonlinear Behaviour of Damping Controlled Fluid-elastic Instability in a Normal Triangular Tube Array. *Journal of Fluids and Structures* **18(5)**: 573-593

Meskell, C., 2004, Numerical estimation of fluid force coefficients in a normal triangular tube array. *Flow Induced Vibration* (de Langre & Axisa ed.), 2004: pp111-116

Meskell, C., 2005, On the underlying fluid mechanics responsible for damping controlled fluidelastic instability in tube arrays. *ASME Pressure Vessels and Piping Division Conference*, Denver *Preprint submitted to Elsevier Science* (M. Pettigrew, N. Mureithi & S. Price)

Mewes, D., Stockmeier, D., Fluid viscosity effects on flow induced vibrations of tube bundles in cross-flow. *Flow Induced Vibrations*, London: I.Mech.E.

S. J. Price, 2001, An investigation on the use of Connors' equation to predict fluidelastic instability in cylinder Arrays, *ASME Journal of Pressure Vessel Technology* **123**: 448–453.

Price, S.J., Paidoussis, M.P., 1984, An improved mathematical model for the stability for the stability of cylinder rows subject to cross-flow. *Journal of Sound and Vibration* **97(4)**: 615-640.

Price, S.J., Zahn, M.L., 1991, Fluidelastic behaviour of a normal triangular array subject to cross flow. *Journal of Fluids and Structures* **5**: 259-278.

Tanaka, H., Takahara, S., 1981, Fluidelastic vibration of tube arrays in cross flow. *Journal of Sound and Vibration* **77**: 19-37.

Weaver, D.S., Yeung, H.C, 1984, The effect of tube mass on the flow induced response of various tube arrays in water. em Journal of Sound and Vibration **93(3)**: 409-425.

Zukaukas, A., 1972, Heat transfer from tubes in cross flow. *Advances in Heat Transfer* **8**: 93-160.